Enhanced Betatron Radiation from a Laser Wakefield Accelerator in a Long Focal Length Geometry

Contact: jonathan.wood08@imperial.ac.uk

J. C. Wood, K. Poder, N. C. Lopes, J. M. Cole, S. Alatabi, C. Kamperidis, S. P. D. Mangles, A. Sahai, Z. Najmudin
The John Adams Institute for Accelerator Science, Blackett Laboratory, Imperial College London, United Kingdom

O. Kononenko, C. A. J. Palmer
DESY, Hamburg, Germany

P. Foster, D. Rusby, D. R. Symes
Central Laser Facility, STFC Rutherford Appleton Laboratory, Chilton, United Kingdom

J. R. Warwick, G. Sarri
Queens University, Belfast, United Kingdom

Abstract

By using a double focal length optic, a 6 m focal length $f/40$ optic compared to a 3 m $f/20$, it was shown that electrons from a self-guiding, self-injecting laser wakefield accelerator, driven by a 120 TW laser pulse, could be accelerated to 1.9 GeV while maintaining a source size below 0.5 µm. Dynamic evolution of the bubble size led to a secondary injection of a high charge per unit bandwidth electron bunch which increased the number of betatron radiation photons by a factor of five at moderate photon energies ($\sim$ 16 keV critical energy). By increasing the laser power to 240 TW the peak brightness of the betatron beam was increased to 3.8×10^{24} photons/s/mm^2/mrad^2/0.1%BW at 18 keV, with the whole beam containing 3×10^{10} photons above 1 keV.

1 Introduction

Laser Wakefield Acceleration (LWFA) [1] is an ultra-high gradient electron acceleration scheme in which electrons gain energy from the large electric fields present in a non-linear plasma wave. A short pulse laser, with a length of half the plasma wavelength λ_p i.e. $c\tau \sim \lambda_p/2$, resonantly excites a plasma oscillation in its wake which has a phase velocity equal to the group velocity of the laser. For an intense laser pulse with a normalised vector potential $a_0 = 0.856 \left(I_{18}{\lambda_{\mu m}}^2\right)^{1/2} \gtrsim 2$, where I_{18} is intensity in units of 10^{18} W/cm^2 and $\lambda_{\mu m}$ is the wavelength in microns, the wake takes the form of an almost spherical bubble that is completely cavitated of electrons [2, 3]. The electric fields inside the bubble exceed 100 GV/m, which is some 3 orders of magnitude higher than the limit of conventional accelerator technology [4]. As these fields travel behind the laser at close to the speed of light, electrons trapped in the bubble experience large accelerating fields for a significant distance, much longer than the plasma wavelength. In a large amplitude wakefield [5], which can be driven by a less intense laser pulse because of pulse self-focussing and self-compression in the plasma [6–9], the fields are large enough to turn around some of the wakefield electrons and trap them in the bubble, in a process called self-injection There are multiple reports of self-injected electron acceleration to GeV energies in cm scale plasmas [10–13], and up to 4.2 GeV in 9 cm [14].

The bubble provides a linear restoring force to off-axis electrons, meaning that any electrons that are injected off-axis or with some transverse momentum oscillate in the bubble at frequency $\omega_\beta = \omega_p/\sqrt{2\gamma}$ where ω_p is the plasma frequency and γ is the Lorentz factor of the electron. These oscillations are called betatron oscillations. The LWFA bubble is, therefore, analogous to a conventional wiggler insertion device, with wiggler parameter $K = \gamma\omega_\beta r_\beta/c$ where r_β is the oscillation radius. As the electrons are highly relativistic the radiation is frequency upshifted by a factor of $2\gamma^2$ in the lab frame. For GeV electron beams from a LWFA, this radiation extends to 10s keV meaning that this is a compact source of hard x-ray radiation. Typically $K \gg 1$ meaning that betatron radiation is broadband. It has been shown theoretically [15] and experimentally [16] that the spectrum is well approximated by the on-axis synchrotron spectrum

$$\frac{d^2I}{dEd\Omega} \propto \gamma^2 \left(\frac{E}{E_c}\right)^2 K_{2/3}^2\left(E/2E_c\right), \tag{1}$$

where $K_{2/3}$ is a modified Bessel function of the second kind. E_c is referred to as the critical energy and can be expressed as

$$E_c = \frac{3\hbar}{4c}\gamma^2{\omega_p}^2 r_\beta. \tag{2}$$

Betatron radiation is emitted from a micron scale source meaning that it is well suited to high resolution imaging in a compact geometry (few metre long beamlines) [17], and also propagation based x-ray phase contrast imaging [18–20]. Betatron radiation has previously been shown to have a peak brightness of a similar order to 3$^{\text{rd}}$ generation synchrotron light sources, with the current record having been set at the Gemini laser with a mean peak brightness $B = (1.2 \pm 0.2) \times 10^{23}$ photons/s/mm^2/mrad^2/0.1%BW at 20 keV [21]. This

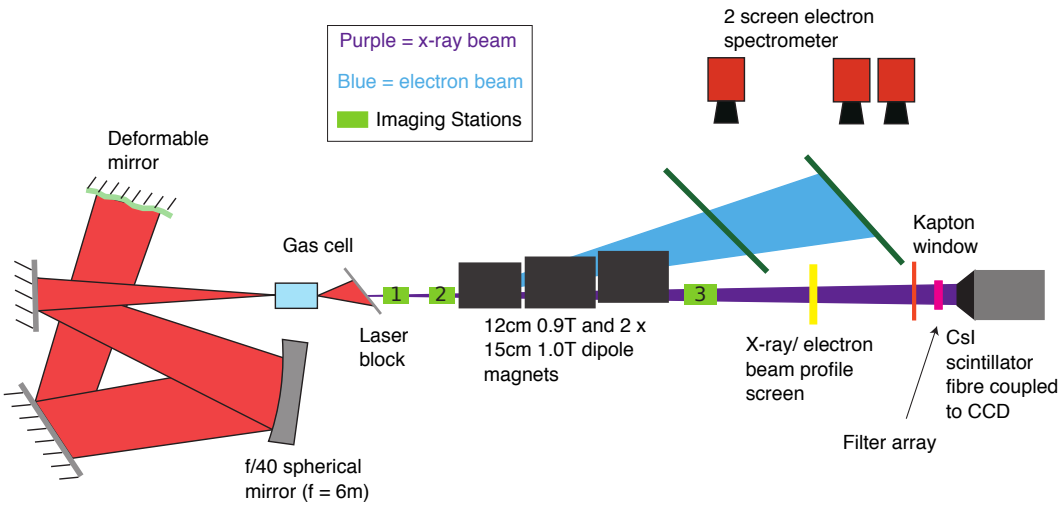

Figure 1: Diagram of the experimental set up.

assumed a 30 fs pulse duration, which is equal to approximately $\lambda_p/(2c)$ at the plasma densities used. The source diameter was $\sim 1.6\,\mu$m.

The high brightness of betatron radiation is largely driven by its small source size and its short pulse length of 10s fs compared to 10-100 ps at synchrotron sources. The number of photons/mrad^2 in the betatron beam is significantly lower: experiments at few hundred TW laser facilities typically produce of order 10^8 to 10^9 photons/shot [13, 21, 22]. Increasing this would improve the signal to noise ratio of betatron x-ray images, which would be particularly useful for imaging rapidly evolving phenomena where multiple shot accumulations are not possible. Additionally by increasing the number of photons/eV betatron radiation could be used to study, in a single shot, the electronic structures of and atomic order in bulk matter via absorption spectroscopy or methods such as EXAFS and XANES [23], or monitor ultrafast phase changes via means of white light Laue diffraction.

2 Experiment

The x-ray energy W_{tot} emitted by electrons of energy $\gamma m_e c^2$ undergoing betatron orbits in a LWFA is given by

$$W_{tot} = \frac{e^2}{6\epsilon_0 c^3} N_e N_\beta {\omega_p}^3 \gamma^{5/2} {r_\beta}^2 \tag{3}$$

where N_e is the number of electrons and N_β is the number of betatron oscillations that each electron undergoes [24]. This has assumed that each electron has the same γ and r_β; typically the peak electron energy is taken as representative of the beam because of the strong $\gamma^{5/2}$ scaling. This scaling suggests that the best way to increase the emitted x-ray energy is to increase γ.

The maximum energy gain W_{max} of electrons in a bubble regime LWFA is given by

$$W_{max} \simeq \frac{2}{3} a_0 \frac{n_c}{n_e} m_e c^2 \tag{4}$$

where n_c is the critical density and n_e is the electron number density [25]. Previous studies have shown that long focal length geometries producing a laser spot size $w_0 > \lambda_p$ allow more energy to be coupled in to a single guided filament, meaning that there is more energy available to drive the wakefield [7]. After self-focussing and self-compression has happened this could lead to a larger a_0 in the bubble, increasing the bubble size and the energy gain. Therefore the 3 m focal length $f/20$ focussing optic used on previous LWFA experiments at Gemini was replaced by a 6 m focal length $f/40$ optic. A diagram of the set up is shown in figure 1.

An $f/40$ spherical mirror focussed the laser pulse to a FWHM spot size of $(54 \pm 2) \times (45 \pm 1)\,\mu$m (after wavefront corrections with the deformable mirror) at the entrance hole of a helium filled adjustable length gas cell. (5.6 ± 0.3) J of 800 nm light were delivered to the target in a nominal pulse length of 47 fs. This corresponds to a peak laser intensity of $(4.1 \pm 0.3) \times 10^{18}$ W/cm^2 and $a_0 = 1.38 \pm 0.05$.

The plasma density inside the gas cell was characterised with a transverse probe beam and a moiré deflectometry diagnostic [26] (not shown). Shortly after the gas cell the transmitted laser light was blocked by a 25 µm thick kapton tape that acted as a plasma mirror and a 24 µm aluminium sheet. The electron beam was swept off-axis by an arrangement of permanent dipole magnets and on to two calibrated Lanex scintillating screens so that its energy spectrum and charge could be determined. The betatron x-ray beam could optionally be detected by an on-axis caesium iodide (CsI) scintillator to measure its spatial profile, or it was allowed to exit the vacuum chamber through a 250 µm thick kap-

ton window where it was detected on a 150 µm thick structured CsI scintillator which was fibre-coupled to a CCD camera. The CsI scintillator plus CCD had been calibrated to provide a conversion from camera counts to x-ray energy deposited in the scintillator [27], so that for a known x-ray spectrum the number of photons could be determined. The critical energy E_c was found by imaging an array of different metal filters placed just before the x-ray camera. Example images can be seen in figure 2. The measured transmission of each of the filters was compared to the calculated transmission of an on-axis synchrotron spectrum for a range of trial values of E_c. The best fit E_c was determined by a least squares fitting to the data.

3 Results

Plasma length scans were performed in the range 3-40 mm at plasma density $n_e = 2.3 \times 10^{18}$ cm^{-3}. The uncertainty in the density retrieved from the moiré diagnostic was $\sim 10\%$, but the shot to shot fluctuation in the backing pressure provided to the cell was significantly lower at 1-2%.

Figure 2 shows example electron beam spectra and x-ray filter array images as a function of gas cell length. The figure shows that over the first 10 mm the first electron beam was injected and accelerated beyond 1.9 GeV before it was dephased i.e. it out-ran the accelerating part of the wakefield, which moves at the group velocity of the laser, and was decelerated. By 10 mm, 100 pC of charge had been accelerated to over 260 MeV, which was the low energy cut-off of the diagnostic. With approximately half of the laser energy, this is double the energy gain that has been previously reported from the same system with an $f/20$ focussing optic [11]. Once the gas cell was extended to 12 mm a second population of electrons was injected. Assuming that the first electron beam did not evolve significantly between 10 and 12 mm (as the second beam obscured its low energy component), the second bunch also contained approximately 100 pC of charge, but with at least four times more charge per MeV. The total electron beam charge did not increase further with accelerator length. Note that after the second injection event the x-ray flux rapidly increased, a phenomenon that will be examined in detail later in this report.

A similar pattern emerged for length scans performed at plasma densities of 2.6, 2.8 and 3.3×10^{18} cm^{-3}. No injection of a second bunch was observed at the lower density of 1.9×10^{18} cm^{-3}, and at 5.7×10^{18} cm^{-3} the beams were so divergent it was not possible to see such details in them. The peak energies of the first and second injected bunches are plotted as a function of gas cell length in figure 3. The errors arise from the uncertainty in the Lanex screen positions relative to the source. This graph confirms that the first electron population is rapidly accelerated to almost 2.0 GeV over the first 10 mm of plasma

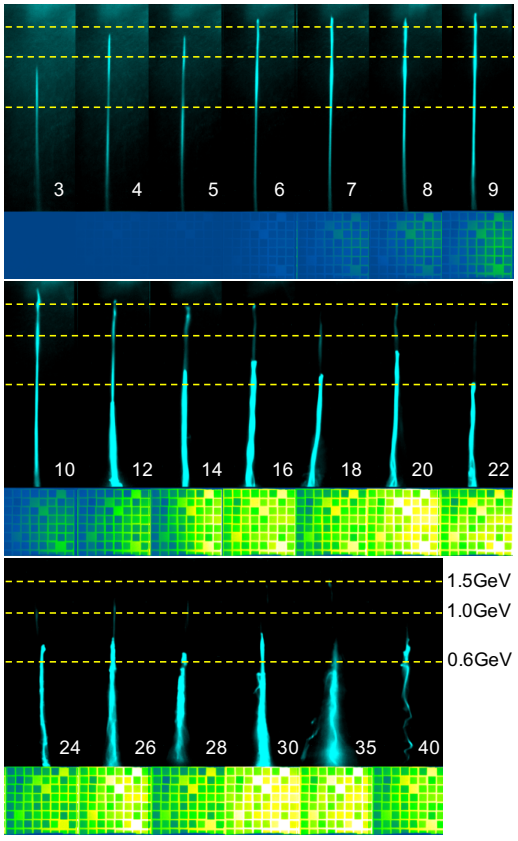

Figure 2: Electron spectra (black/blue) and x-ray filter array images (green) from a plasma length scan, with length in mm denoted by the white numbers. The electron spectra are images of the scintillating screens after the electron beam had been dispersed by the magnet. Vertical position on the image is related to the electron's energy, and the horizontal coordinate is proportional to the beam divergence. The filter array images were used to calculate the critical energy. Lighter green indicates a higher x-ray flux.

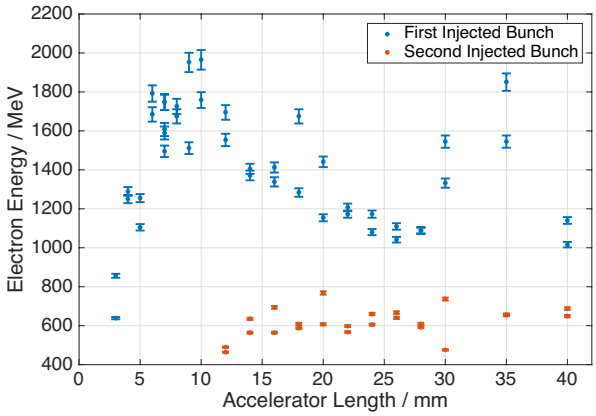

Figure 3: Peak energies of the first and second injected electron bunches.

at which point it starts to dephase. Very shortly after this happens, between 10 and 12 mm, the second population of electrons was injected and accelerated to a peak energy of 600-700 MeV, which did not increase further with accelerator length.

A 2D particle-in-cell simulation was performed with the EPOCH code [28] to explore this behaviour. 25 and 10 cells per laser wavelength were used in the propagation and transverse directions respectively. In the simulation a laser pulse with a slightly enhanced $a_0 = 1.90$, with a FWHM duration of 49 fs and FWHM spot size of 44 µm was focussed in to an initially uniform plasma with $n_e = 2.5 \times 10^{18}$ cm^{-3}. a_0 was increased slightly compared to the experiment because pulse self-focussing happens more slowly in 2D. The plasma length was 34 mm and had 0.5 mm linear density ramps at each end. The laser was focussed at the top of the density up ramp. The simulation showed that the first beam is self-injected after $\sim$ 1.4 mm and accelerated beyond 1.0 GeV. Then after a period of pulse self-focussing and self-compression the bubble was greatly lengthened, as demonstrated in figure 4, which led to an injection of a high charge electron bunch as previously theorised in [29][30]. Shortly after

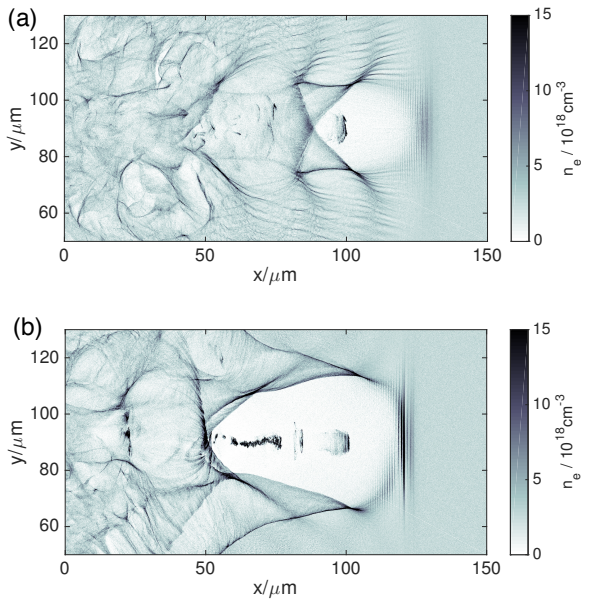

Figure 4: PIC simulation outputs of electron number density (a) shortly after the first injection of charge 2 mm in to the plasma and (b) shortly after the second injection of charge 5.9 mm in to the plasma.

the secondary injection the laser depleted significantly and the bubble length contracted, which limited the energy gain of these electrons. The experimental results demonstrate that this dynamic mechanism is remarkably reproducible despite shot-to-shot fluctuations in laser intensity, and over a range of plasma densities.

Figure 2 also demonstrated that the characteristics of the betatron radiation were dramatically altered by the injection of this second bunch of electrons. We first examine the critical energy E_c as a function of accelerator length, which is plotted in figure 5. As expected, be-

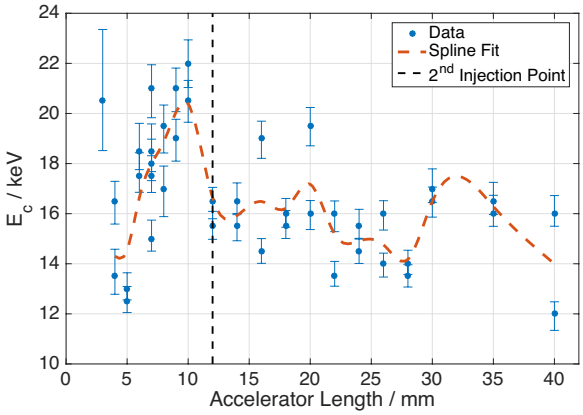

Figure 5: E_c as a function of plasma length. The black dashed line marks the secondary injection point, and the red dashed line is a spline fit to the data.

fore the second injection E_c increased with accelerator length as the peak γ of the electron spectrum increased. When the second bunch was injected at 12 mm accelerator length there was a sudden decrease in the critical energy. This suggests that the second bunch, which had a much lower γ^2, was contributing significantly to the overall x-ray spectrum by reducing its apparent temperature. After the injection of the second bunch there was little change in the spectral shape, as expected from the electron results.

An estimate of the betatron oscillation radius can be made using equation 2 because E_c, ω_p and the electron beam energy spectra are known. Taking the peak γ from figure 3, r_β's in the range $100-200$ nm were found for accelerator lengths between 6 and 10 mm. This is amongst the lowest reported source sizes in the literature [31], and lower than what has been observed in other self-guided experiments [22, 32].

By combining the number of counts on the calibrated x-ray camera to the measured FWHM beam divergence, which varied linearly between 3 and 14 mrad between densities of 1.9 and 3.3 $\times$ 10^{18} cm^{-3} (it was 8 mrad at $n_e = 2.3 \times 10^{18}$ cm^{-3}), the total number of photons in the beam was estimated, and is shown as a function of accelerator length in figure 6. Within 2 mm of the second injection the total number of photons increased by a factor of 5 to approximately 5×10^9: fifty times larger than what was reported in [22]. Comparing this behaviour to that of E_c in figure 5, it is clear that the second bunch radiated a large number of moderate energy photons. The photon number increase is surprising in light of equation 3 because of the significantly lower energy gain of this bunch. Therefore the oscillation radius of this bunch must be much larger. An estimate for this radius, $r_{\beta 2}$, can be found by fitting a

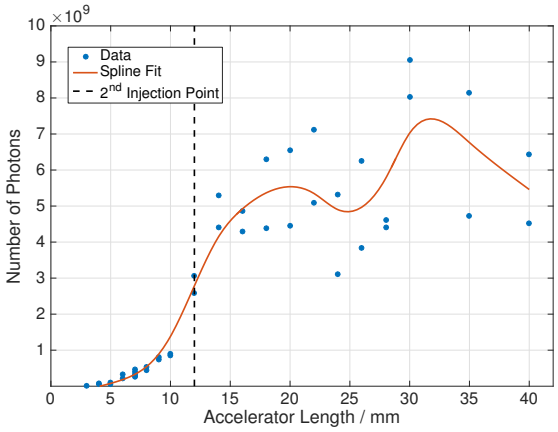

Figure 6: Total number of photons as a function of accelerator length.

two-temperature spectrum to the E_c data. At 12 mm, where the first bunch has just started to dephase, the x-ray spectrum from the first bunch was assumed to be the same as that at 10 mm, where $E_c = (21 \pm 1)\,\mathrm{keV}$. There was approximately a tripling in the total number of x-ray photons when the second bunch was injected. When this happened the measured E_c, assuming a single on-axis synchrotron spectrum, fell to $(16 \pm 1)\,\mathrm{keV}$. This total spectrum can, therefore, be approximated by the sum:

$$A\ S(E, 21\mathrm{keV}) + 2A\ S(E, E_{c2}) = 3A\ S(E, 16\mathrm{keV}) \quad (5)$$

A is related to the amplitude of the spectrum of the first injected bunch and $S(E, E_c)$ is the on-axis synchrotron spectrum, where each has been normalised such that the integral over all energies is 1. We now find E_{c2} from a range of trial values that minimises the squared difference between the integral over all energy of the left and right hand sides of this equation. This produces a best fit $E_{c2} \approx 7.3\,\mathrm{keV}$. Combining this with the peak electron energy from figure 3, of approximately 480 MeV, suggests $r_{\beta 2} \sim 700\,\mathrm{nm}$.

This estimate of the oscillation radius of the second bunch allows for a simple check calculation on the number of photons. The number of electrons N_e is doubled by the second injection and r_β increases by a factor of $\sim 700/150 = 4.7$. The number of oscillations per electron $N_\beta \sim L/\lambda_\beta$ where L is the acceleration length. At 20 mm acceleration length the first bunch had been accelerated for $\sim$ 20 mm to a $\gamma \sim 3000$, and the second bunch had been accelerated for $\sim$ 8 mm to $\gamma \sim 1200$. Therefore $N_{\beta 1} \sim 12$ and $N_{\beta 2} \sim 7$. From equation 3, the ratio of the total emitted energy by the second bunch to that of the first bunch was ~ 2.6. Converting this value in to a number of photons using the estimated spectra emitted by each electron beam produced ratio of the number of photons emitted by the second bunch to the first bunch of ~ 6.6. Figure 6 shows an increase in photon number by a factor of $5 - 6$, which is in reasonable agreement with the estimate considering the number of approximations that have been made.

In figure 7 brightness is plotted as a function of accelerator length. For lengths below 12 mm the source

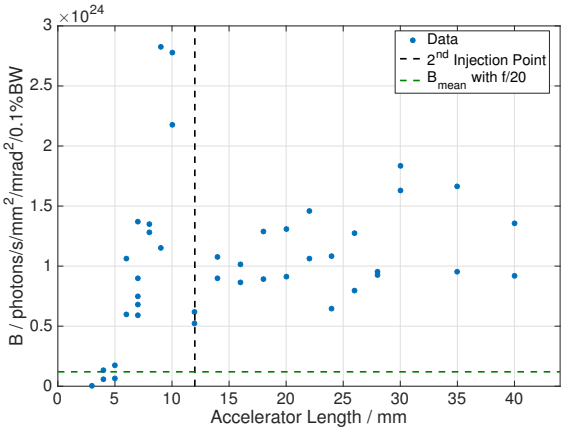

Figure 7: Brightness as a function of accelerator length. The green dashed line shows the mean peak brightness with an $f/20$ geometry

radius was calculated from equation 2. Above 12 mm $r_\beta = 0.5\,\mu\mathrm{m}$ was assumed owing to the difficulties of attributing an effective r_β from the two spectra. However this does lie between $r_{\beta 1}$ and $r_{\beta 2}$. At short accelerator lengths, a very high brightness is driven by a small source size. The maximum peak brightness recorded was $2.8 \times 10^{24}\,\mathrm{photons/s/mm^2/mrad^2/0.1\%BW}$, a factor of 23 higher than the mean peak brightness from earlier Gemini experiments, and a factor of 7.5 higher than the brightest ever shot recorded in an $f/20$ configuration. After the second injection the high brightness was reduced by the larger source size, but remained around 10 times larger than previous measurements because of the dramatic increase in photon flux with the injection of the second electron population.

By approximately doubling the laser energy on target a_0 was increased to 1.85 ± 0.07. In the high photon regime (i.e. after the second injection of charge) slightly harder betatron beams with $E_c = (18.0 \pm 0.6)\,\mathrm{keV}$ were produced containing up to 3×10^{10} photons in the whole beam above 1 keV. The peak brightness recorded was $3.8 \times 10^{24}\,\mathrm{photons/s/mm^2/mrad^2/0.1\%BW}$. This was driven by the large number of photons/mrad^2/eV meaning that this increase could have a large impact on studies relying on this metric, including imaging, absorption and diffraction based experiments.

4 Conclusion

By doubling the focal length of the laser pulse it was shown that electrons could be accelerated to 1.9 GeV in a self-guided, self-injecting LWFA, compared to approx-

imately 1 GeV in the shorter focal length case. Spectral measurements of the betatron emission revealed that the oscillation radius of these electrons was of order 100-200 nm, which contributed to the very high peak brightness of the betatron emission, up to 2.8×10^{24} photons/s/mm^2/mrad^2/0.1%BW with a critical energy of 21 ± 1 keV.

At longer acceleration lengths, a rapid expansion of the bubble size caused by self-focussing and self-compression of the laser pulse led to a second injection of electrons with four times as much charge per MeV. The second bunch caused a five-fold increase in the number of photons along with a decrease in the effective critical energy to ~ 16 keV, caused by a combination of its larger oscillation radius and lower peak energy. By increasing the laser power from 120 TW to 240 TW the brightness in the high photon flux regime was increased to 3.8×10^{24} photons/s/mm^2/mrad^2/0.1%BW at 18 keV, with the whole beam containing 3×10^{10} photons with energies > 1 keV. This is a significantly higher brightness and photon flux than has been previously reported in the literature.

5 Acknowledgements

The authors are grateful to the CLF facility staff for their hard work and dedication. We acknowledge funding from STFC for the support of the John Adams Institute of Accelerator Science by grants ST/J002062/1 and ST/P000835/1. The EPOCH code used in this research was developed under UK Engineering and Physics Sciences Research Council grants EP/G054940/1, EP/G055165/1 and EP/G056803/1.

References

[1] T. Tajima et al., *Laser Electron Accelerator*, Phys. Rev. Lett. 4(4), pp. 267-270, 1979.

[2] A. Pukhov et al., *Laser wake field acceleration: the highly non-linear broken-wave regime*, Appl. Phys. B Lasers Opt. 74(4-5), pp. 355-361, 2002.

[3] W. Lu et al., *Nonlinear Theory for Relativistic Plasma Wakefields in the Blowout Regime*, Phys. Rev. Lett. 96(16), p. 165002, 2006.

[4] K. Poder et al., *Multi-GeV Electron Acceleration in Strongly Non-Linear Wakefield Driven by Oversized Laser Spots*. In preparation, 2017.

[5] S. P. D. Mangles et al., *Self-injection threshold in self-guided laser wakefield accelerators*, Phys. Rev. Spec. Top. - Accel Beams 15(1), p. 011302, 2012.

[6] W. Mori, *The physics of the nonlinear optics of plasmas at relativistic intensities for short-pulse lasers*, IEEE J. Quantum Electron. 33(11), pp. 1942-1953, 1997.

[7] A. G. R. Thomas et al., *Effect of Laser-Focusing Conditions on Propagation and Monoenergetic Electron Production in Laser-Wakefield Accelerators*, Phys. Rev. Lett. 98, p. 095004, 2007.

[8] R. Wagner et al., *Electron Acceleration by a Laser Wakefield in a Relativistically Self-Guided Channel*, Phys. Rev. Lett. 78(16), pp. 3125-3128, 1997.

[9] J. Faure et al., *Observation of Laser-Pulse Shortening in Nonlinear Plasma Waves*, Phys. Rev. Lett. 95(20), p. 205003, 2005.

[10] W. P. Leemans et al., *GeV electron beams from a centimetre-scale accelerator*, Nat. Phys. 2(10), pp. 696-699, 2006.

[11] S. Kneip et al., *Near-GeV Acceleration of Electrons by a Nonlinear Plasma Wave Driven by a Self-Guided Laser Pulse*, Phys. Rev. Lett. 103(3), p. 035002, 2009.

[12] H. T. Kim et al., *Enhancement of Electron Energy to the Multi-GeV Regime by a Dual-Stage Laser-Wakefield Accelerator Pumped by Petawatt Laser Pulses*, Phys. Rev. Lett. 111(16), p. 165002, 2013.

[13] X. Wang et al., *Quasi monoenergetic laser plasma acceleration of electrons to 2 GeV*, Nat. Commun. 4:1988, 2013.

[14] W. P. Leemans et al., *Multi-GeV Electron Beams from Capillary-Discharge-Guided Sub-petawatt Laser Pulses in the Self-Trapping Regime*, Phys. Rev. Lett. 113(24), p. 245002, 2014.

[15] E. Esarey et al., *Synchrotron radiation from electron beams in plasma-focusing channels*, Phys. Rev. E. 65(5), p. 056505, 2002.

[16] S. Fourmaux et al., *Demonstration of the synchrotron-type spectrum of laser-produced Betatron radiation*, New Journal of Physics 13(3), p. 033017, 2011.

[17] J. M. Cole et al., *Laser-wakefield accelerators as hard x-ray sources for 3D medical imaging of human bone*, Sci. Rep. 5, p. 13244, 2015.

[18] S. Kneip et al., *X-ray phase contrast imaging of biological specimens with femtosecond pulses of betatron radiation from a compact laser plasma wakefield accelerator*, Applied Physics Letters 99(9), p. 093701, 2011.

[19] S. Fourmaux et al., *Single shot phase contrast imaging using laser-produced Betatron x-ray beams*, Opt. Lett. 36(13), pp. 2426-2428, 2011.

[20] J. Wenz et al., *Quantitative X-ray phase-contrast microtomography from a compact laser-driven betatron source*, Nat. Commun. 6:7568, 2015.

[21] M. S. Bloom et al., *Hard X-rays Produced by Betatron Motion of Self Injected Electrons in a Laser Wake Field Accelerator*. In preparation, 2017.

[22] S. Kneip et al., *Bright spatially coherent synchrotron X-rays from a table-top source*, Nat. Phys. 6(12), pp. 980-983, 2010.

[23] F. Albert et al., *Laser wakefield accelerator based light sources: potential applications and requirements*, Plasma Phys. Control. Fusion 56(8), p. 084015, 2014.

[24] John D. Jackson *Classical Electrodynamics*, Third Edition, p. 666.

[25] W. Lu et al., *Generating multi-GeV electron bunches using single stage laser wakefield acceleration in a 3D nonlinear regime*, Phys. Rev. Spec. Top. - Accel. Beams 10(6), p. 061301, 2007.

[26] I. Glatt et al., *Moire Deflectometry - Ray Tracing lnterferometry*, Optics and Lasers in Engineering 8, pp. 277-320, 1988.

[27] J. C. Wood et al., *Calibration of the CLF Andor iKon Indirect Detection Camera*, CLF Annual Report, 2017.

[28] T. D. Arber et al., *Contemporary particle-in-cell approach to laser-plasma modelling*, Plasma Phys. Control. Fusion 57(11), p. 113001, 2015.

[29] S. Kalmykov et al., *Electron Self-Injection and Trapping into an Evolving Plasma Bubble S.*, Phys. Rev. Lett. 103, p. 135004, 2009.

[30] S. Yi et al., *Hamiltonian analysis of electron self-injection and acceleration into an evolving plasma bubble*, Plasma Phys. Control. Fusion 53(1), p. 014012, 2011.

[31] G. R. Plateau et al., *Low-Emittance Electron Bunches from a Laser-Plasma Accelerator Measured using Single-Shot X-Ray Spectroscopy*, Phys. Rev. Lett. 109(6), p. 064802, 2012.

[32] M. Schnell et al., *Deducing the electron-beam diameter in a laser-plasma accelerator using x-ray betatron radiation*, Phys. Rev. Lett. 108, p. 075001, 2012.